Landscapes of Santa Rosa Island, Channel Islands National Park, California

Authors: Schumann, R. Randall, Minor, Scott A., Muhs, Daniel R., and Pigati, Jeffrey S.

Source: Monographs of the Western North American Naturalist, 7(1) : 48-67

Published By: Monte L. Bean Life Science Museum, Brigham Young University

URL: https://doi.org/10.3398/042.007.0108

LANDSCAPES OF SANTA ROSA ISLAND, CHANNEL ISLANDS NATIONAL PARK, CALIFORNIA

R. Randall Schumann[1,2], Scott A. Minor[1], Daniel R. Muhs[1], and Jeffrey S. Pigati[1]

ABSTRACT.—Santa Rosa Island (SRI) is the second-largest of the California Channel Islands. It is one of 4 east–west aligned islands forming the northern Channel Islands chain, and one of the 5 islands in Channel Islands National Park. The landforms, and collections of landforms called landscapes, of Santa Rosa Island have been created by tectonic uplift and faulting, rising and falling sea level, landslides, erosion and deposition, floods, and droughts. Landscape features, and areas delineating groups of related features on Santa Rosa Island, are mapped, classified, and described in this paper. Notable landscapes on the island include beaches, coastal plains formed on marine terraces, sand dunes, and sand sheets. In this study, the inland physiography has been classified into 4 areas based on relief and degree of fluvial dissection. Most of the larger streams on the island occupy broad valleys that have been filled with alluvium and later incised to form steep- to vertical-walled arroyos, or barrancas, leaving a relict floodplain above the present channel. A better understanding of the processes and mechanisms that created these landscapes enhances visitors' enjoyment of their surroundings and contributes to improving land and resource management strategies in order to optimize and balance the multiple goals of conservation, preservation, restoration, and visitor experience.

RESUMEN.—La Isla Santa Rosa (ISR) es la segunda isla más grande de las Islas del Canal de California. Es una de las cuatro islas alineadas de este a oeste que forman la cadena norte de las Islas del Canal y es una de las cinco islas del Parque Nacional Islas del Canal. Las formas del relieve, y las colecciones de accidentes geográficos llamados paisajes, de la Isla Santa Rosa fueron creadas por movimientos y fallas tectónicas, la elevación y la disminución del nivel del mar, deslizamientos de tierra, erosión y deposición, inundaciones y sequías. En este artículo designamos, clasificamos y describimos las características del paisaje y las áreas que delimitan grupos de rasgos relacionados de la Isla Santa Rosa. Notables paisajes de la isla incluyen playas, llanuras costeras formadas por terrazas marinas, dunas de arena y llanuras de arena. En este estudio, hemos clasificado la fisiografía tierra adentro en cuatro áreas basadas en el desagüe y el grado de disección fluvial. La mayor parte de las corrientes de agua más grandes ocupan amplios valles que han sido rellenados con aluvión y cortados más tarde para formar arroyos inclinados o verticales, o barrancas, dejando un relicto de una planicie aluvial por encima del canal actual. Una mejor comprensión de los procesos y mecanismos que crearon estos paisajes hace que el visitante disfrute más del paisaje que le rodea, y contribuye a mejorar las estrategias de gestión de la tierra y los recursos para optimizar y equilibrar los múltiples objetivos de conservación, preservación, restauración y experiencia del visitante.

Santa Rosa Island (SRI) is the second largest of the California Channel Islands (Fig. 1), measuring approximately 25 km long and 16 km wide, with an area of 215 km². It is part of the group of 4 east–west aligned islands that make up the northern Channel Islands chain, located roughly 50 km southwest of Santa Barbara and 70 km west of Oxnard, California. SRI is one of the 5 islands in Channel Islands National Park.

Santa Rosa Island has a maritime Mediterranean climate, with cool, rainy winters and warm, dry summers. Air temperatures on the island rarely exceed 30 °C or fall below 10 °C. Fog is a common occurrence in the summer months and constitutes an important source of moisture for plants (e.g., Williams et al. 2008).

Modern vegetation types include coastal sage scrub, island chaparral, grassland, and scattered oak and pine woodlands (Junak et al. 2007), but prior to about 9000 years ago, a cooler, more humid climate supported extensive pine, fir, and cypress forests (Anderson et al. 2010).

Human occupation of Santa Rosa Island dates back at least 13,000 calendar years (Johnson et al. 2000). By the time of first European contact by Juan Rodrigues Cabrillo in 1542, the native Chumash people on Santa Rosa Island numbered in the hundreds, living in at least 9 coastal villages (Kennett 2005). Chumash society flourished on the Channel Islands until the early 1800s, when the native people were removed from the islands and brought

[1]United States Geological Survey, Box 25046, MS 980, Denver Federal Center, Denver, CO 80225-0046.
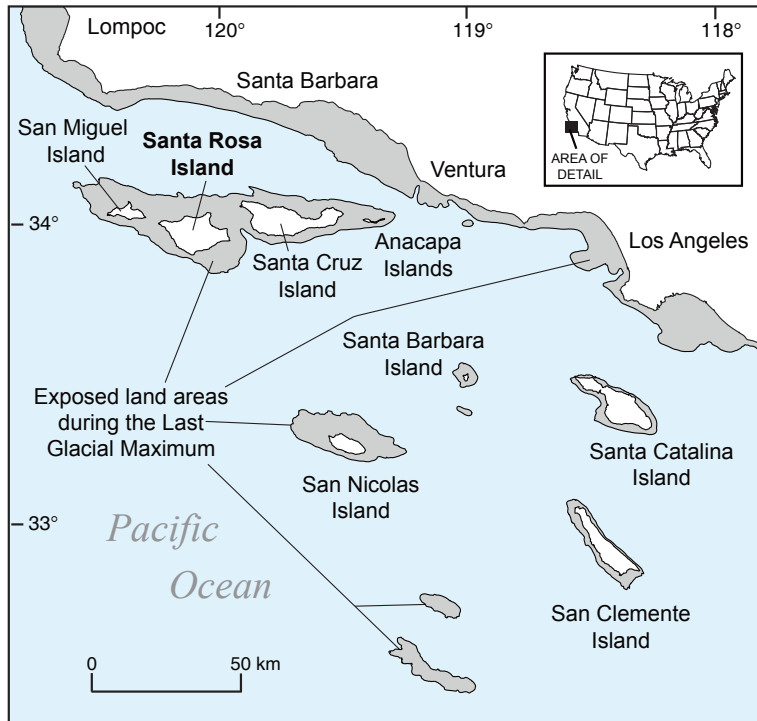[2]E-mail: rschumann@usgs.gov

Fig. 1. Location of the California Channel Islands. Also depicted are land areas that were exposed during the Last Glacial Maximum, when sea level was approximately 95 m lower than present (Muhs et al. 2012). San Miguel, Santa Rosa, Santa Cruz, Anacapa, and Santa Barbara islands make up Channel Islands National Park.

to mainland Spanish missions (Johnson and McLendon 2000).

European settlement of Santa Rosa Island began in 1843 when the governor of Mexico granted the island to Jose and Carlos Carrillo (Allen 1996). In 1844, the Carrillo brothers brought sheep, cattle, and horses to the island, thus initiating the ranching era. By the 1860s, the island had been sold to the More family, who increased the number of sheep to about 100,000. In 1901, the Vail and Vickers Company purchased the island and converted it from a sheep ranch to a cattle ranch (Allen 1996). Deer and elk were brought to the island for hunting in the 1920s (the last ungulates were removed in 2011). In 1986, the National Park Service purchased the island from Vail and Vickers, adding Santa Rosa to the islands of Channel Islands National Park.

The landforms, and collections of landforms called landscapes, of Santa Rosa Island have been created by the forces of climate and geology acting over the past few millions of years. Tectonic uplift and faulting, rising and

falling sea level, landslides, erosion and deposition, floods, and droughts have acted to shape the island's mountains, valleys, plains, beaches, cliffs, dunes, and other landforms. In this paper, we characterize and describe these landforms in the context of the physical processes that are responsible for their creation.

GEOLOGIC SETTING

Santa Rosa Island and the other 3 northern Channel Islands are the emergent parts of an approximately 125 km long platform that, along with the Santa Monica Mountains to the east, forms the southern part of the western Transverse Ranges crustal block (Crouch 1979, Vedder and Howell 1980). Approximately 2000 m of mostly marine shale, siltstone, sandstone, conglomerate, and volcaniclastic rocks of Eocene to Miocene age, with local volcanic flows and shallow intrusions, are exposed on Santa Rosa Island (Avila and Weaver 1969, Weaver and Doerner 1969, Dibblee and Eherenspeck 1998). Most of the pre-Pleistocene rocks were
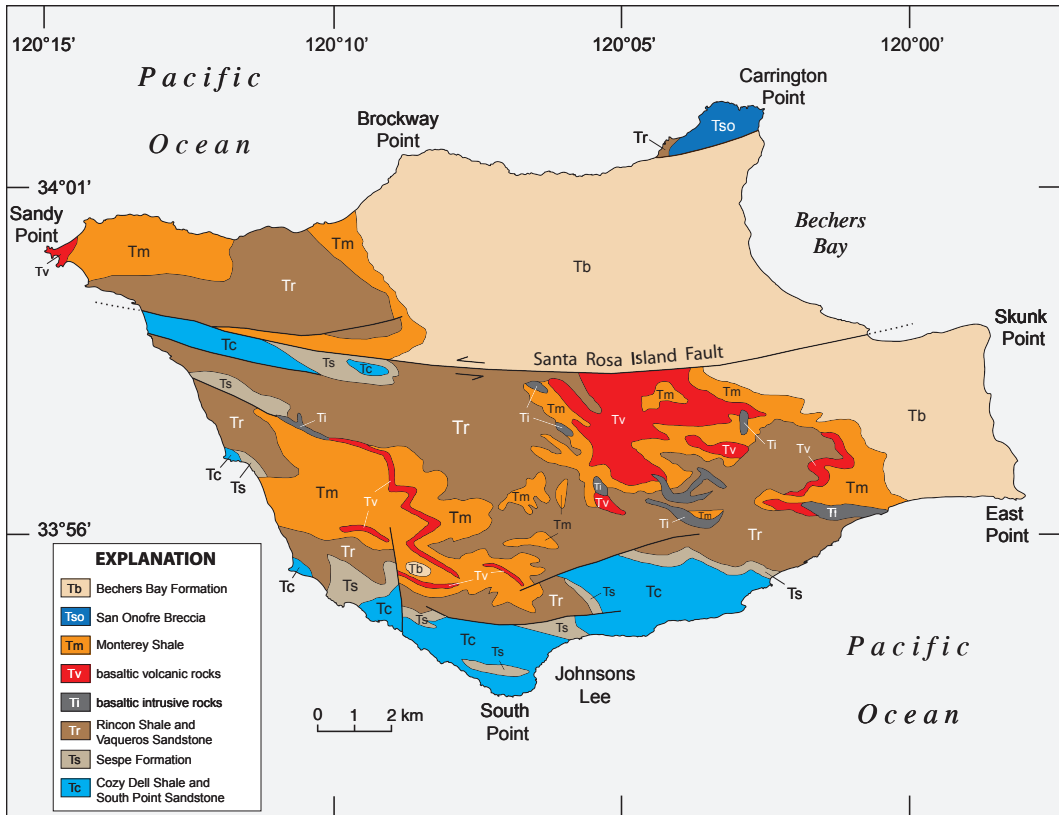
Fig. 2. Simplified geologic map of Santa Rosa Island (after Dibblee and Eherenspeck 1998). All units shown are of Tertiary (Eocene to Miocene) age. Quaternary deposits, including marine terrace deposits, eolian sand, and river alluvium, are not shown.

deposited in shallow- to deep-water ocean environments that predated the island's emergence. The oldest rock units are exposed in the southern and western parts of the island and are overlain by progressively younger units to the north and northeast (Fig. 2).

Pleistocene and Holocene surficial deposits include colluvium and alluvium on the slopes and floors of valleys; eolian sands; marine-terrace deposits, some of which form narrow coastal plains; and modern beach sands (Dibblee and Eherenspeck 1998, Woolley 1998). Landslides are common in many areas, particularly on steeper slopes in the southern and central parts of the island.

The island is bisected by the roughly east–west striking, subvertical to steeply north-dipping Santa Rosa Island Fault (SRIF). Left-lateral strike-slip movement along the fault has caused the northern part of the island to move west, or left, relative to the southern part, giving

Santa Rosa Island its distinctive "parallelogram" shape (Fig. 2). Estimates of the amount of strike-slip movement along the fault, based on displacement of rock units, range from 5.5 km (Nuccio and Woolley 1998) to 16 km (Weaver 1969). Drainages that cross the fault are deflected as much as 1 km to the west, reflecting relatively recent (late Pleistocene and/or Holocene) lateral movement. Displacement of bedrock units suggests that the SRIF has also experienced vertical displacement. Older rocks on the south side of the fault are juxtaposed against younger rocks north of the fault (Fig. 2), suggesting that the south side of the fault has moved upward relative to the north side. Vertical offset of as much as 400 m can be inferred from geologic cross sections (e.g., Dibblee and Eherenspeck 1998). South-side-up displacement is also suggested by the topography; elevations are generally higher south of the fault, and the island's main drainage
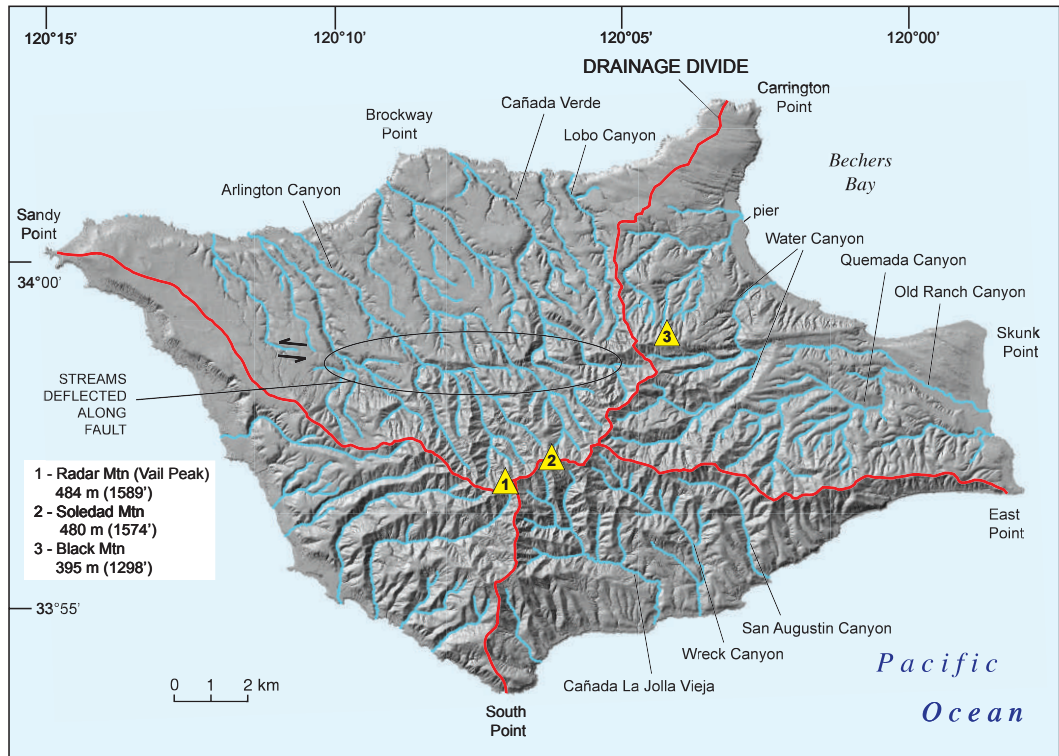
Fig. 3. Shaded relief map of Santa Rosa Island showing drainage divides (red lines), high points (yellow triangles), and locations of selected features. Note 1 km or more of offset of drainages crossing the Santa Rosa Island fault.

divide is located well south of the island's center (Fig. 3). However, evidence of more recent fault displacement that resulted in relative uplift of the north side of the SRIF has been presented, including (1) up-to-the-north offset of last interglacial (~80–120 ka; ka = thousands of years before present) marine terraces on the east end of the island (Sorlien 1994, Pinter et al. 2001); (2) a prominent south-facing escarpment on the north side of the fault between Bechers Bay and Arlington Canyon, which is highest at Black Mountain (Fig. 3); and (3) dip-slip striae preserved on principal slip surfaces in multiple exposures of the fault, indicating that the most recent movement has been up-to-the-north in the eastern part of the island (Minor et al. 2012). The SRIF is the only fault that crosses the entire island. A number of secondary faults run subparallel to the SRIF (Fig. 2).

LANDSCAPES

Individual landforms on Santa Rosa Island, such as mountains, valleys, and plains, give the landscape its character. These features, and areas delineating distinct landscapes composed of these landforms have been mapped and classified (Fig. 4), and are described below.

Coastal Plains (Marine Terraces)

Marine terraces are emergent, flat to gently seaward-sloping erosional platforms veneered with thin, sometimes fossil-bearing shallow-water marine sand and gravel, backed by a relatively steeper sea cliff at their landward margins. Marine terrace landforms and their associated sedimentary deposits and fossils record the combined effects of tectonic uplift and glacio-eustatic fluctuations of global sea level. The intersection of the marine terrace platform with the base of the sea cliff, called the shoreline angle, records the position and elevation of the paleo-shoreline, after adjusting for tectonic and isostatic movements that occurred since the shoreline occupied that position (Lajoie 1986, Muhs et al. 2002). Fossil mollusk shells and corals are used to date the deposits by use of direct methods, including
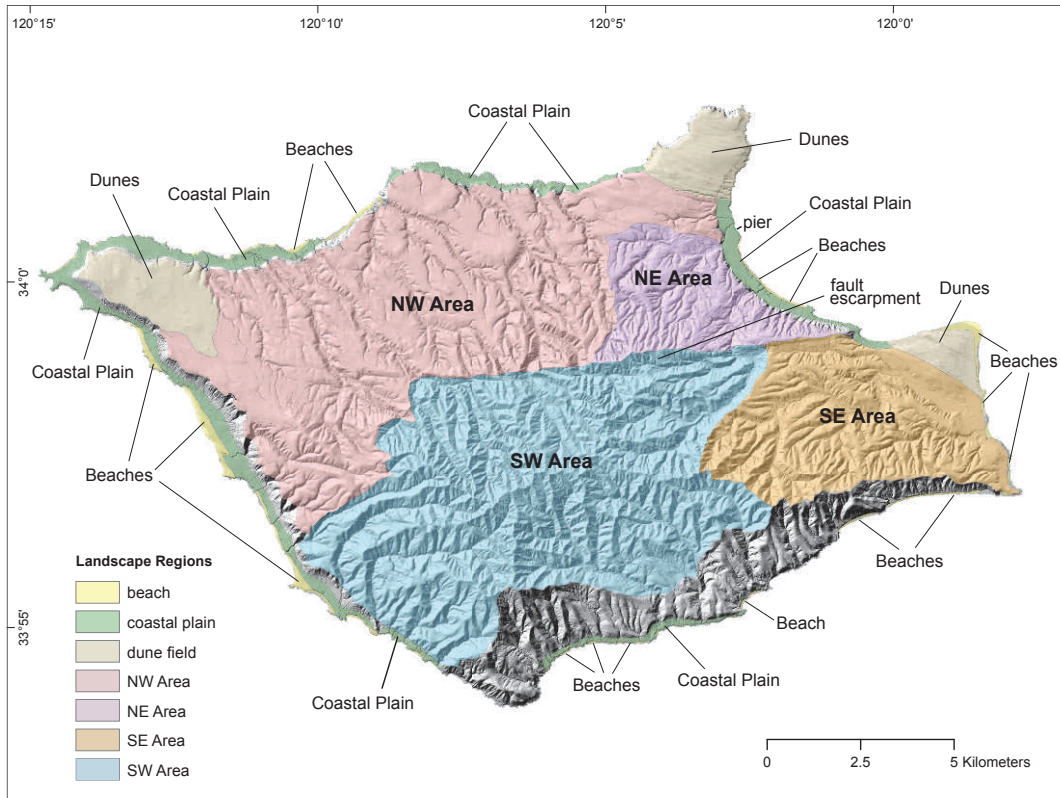
Fig. 4. Landscape regions of Santa Rosa Island. Areas are delineated on the basis of terrain characteristics, including topographic ruggedness and drainage density, as discussed in text. The gray areas comprising coastal slopes are not discussed in this paper.

radiocarbon and uranium-series disequilibrium, as well as indirect methods such as strontium isotope ratios and amino acid racemization (Muhs et al. 2004).

In tectonically stable areas, only terraces formed by past sea levels that were higher than present are preserved on land areas. On uplifting coastlines, however, marine terrace landforms and deposits of many high sea stands can be preserved, including those that may have formed below present sea level. In areas that have experienced relatively continuous uplift throughout the Pleistocene, such as coastal southern California and the Channel Islands, the youngest marine terraces are those closest to sea level, and successively higher terraces are successively older. The terrace surfaces are typically covered with a relatively thin layer of coastal dune sand, alluvium, or colluvium that may generally reflect the shape of the original terrace platform, such as the

last interglacial (~120–80 ka) marine terrace surrounding Bechers Bay (Fig. 5A, 5B). In other places, marine terraces may be mostly buried and obscured by younger deposits so that the only visible evidence of their presence are underlying marine sand and gravel layers exposed along roadcuts, hillslopes, or river valleys. One example of an older (probably >1 Ma; Ma = millions of years before present) marine terrace deposit with no topographic expression is exposed in a roadcut along Main Road on the slopes of Black Mountain (Fig. 5C).

Marine terraces are prominent geomorphic features on Santa Rosa Island. Orr (1960) identified at least 3 distinct marine terrace surfaces on the island, whereas Pinter et al. (2001) mapped 4 terraces based on their visible geomorphic expression. Near the present-day shoreline, last-interglacial marine terrace surfaces covered by alluvium and/or eolian sand form relatively flat to seaward-sloping coastal
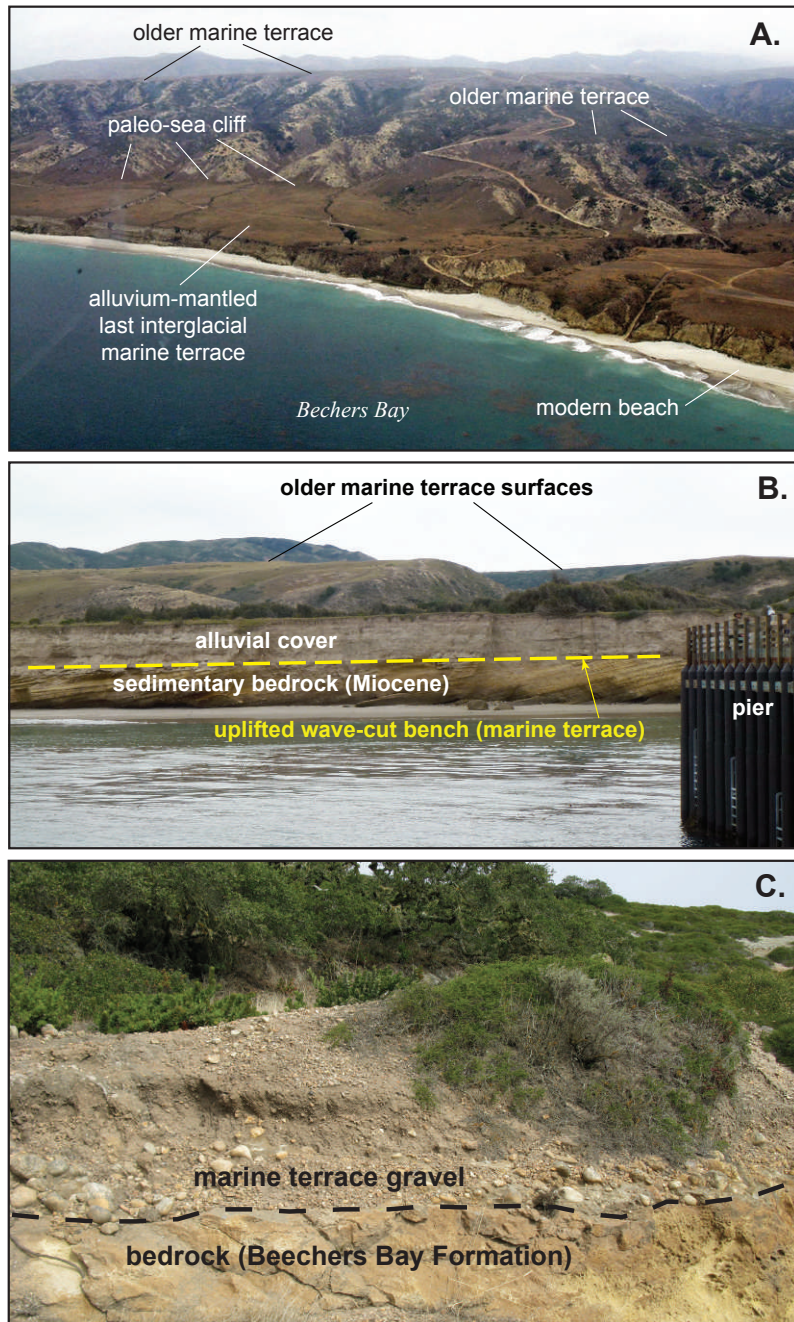
Fig. 5. (A) Marine terraces along Bechers Bay, aerial view looking southward. (B) Marine terrace stratigraphy in sea-cliff face in Bechers Bay, as seen from the pier (right side of photo). (C) Marine terrace deposits along Main Road near Black Mountain.

plains, particularly on the north, east, and west sides of the island (Fig. 4). Around Bechers Bay, the wave-eroded last-interglacial marine-terrace surface separates dipping sandstone bedrock below from its cover of subhorizontally bedded alluvium and colluvium above, which is easily seen in the face of the sea cliffs when approaching the island (Fig. 5B). The upland

Fig. 6. Aerial view of ancient marine terrace surface in the NW Area, looking southward across the island. LIG = last interglacial.

surface of the northern half of the island is a dissected older marine terrace or series of terraces mantled by eolian sand and alluvium (Fig. 6; Orr 1960, 1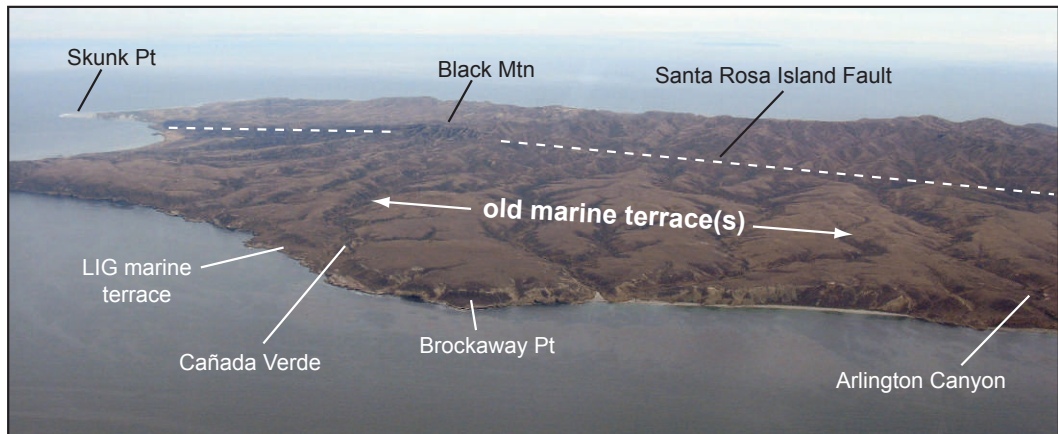967, Pinter et al. 2001). Over time, as this terrace was uplifted, as much as several tens of meters of windblown sand covered parts of the original terrace benches, and rivers cut into its surface (Woolley 1998).

Sand Dunes and Eolian Sand Sheets

Eolian (windblown) sand deposits are prominent features on the outer Channel Islands. On Santa Rosa Island, extensive dune fields are present at Sandy Point, Carrington Point, and Skunk Point (Fig. 4). A veneer of windblown sand ranging from a few centimeters to several tens of meters thick also covers the upland surfaces of much of the island north of the SRIF. Most of the sand is white to light gray in color, as opposed to the tan to light brown color of the quartz- and feldspar-dominated sands common to the mainland coast. In contrast to sand derived primarily from erosion of sandstone bedrock, eolian sand on SRI and the other Channel Islands is derived from eroded fragments of marine-invertebrate skeletal material that is composed largely of white to light gray calcium carbonate (Muhs et al. 2009). These sands were blown onshore primarily during glacial periods, when sea level around southern California and the Channel Islands was much lower than today. For example, at the peak of the last glacial period, about 24,000–20,000 calendar years ago, sea level was approximately 95 m lower than today

(Muhs et al. 2012), exposing large areas of the submarine shelves surrounding the Channel Islands (Fig. 1). Prevailing winds from the northwest deflated (eroded) the carbonate sands from the shelves and blew them onto what is presently the land areas. During interglacial periods, sea level rose, submerging the shelf areas and cutting off the sand supply, thus allowing the dunes to stabilize (Muhs et al. 2009). Most eolian deposits on SRI have been stabilized by vegetation or cementation, but a few areas of partially active dunes are still present, such as the climbing dunes near Skunk Point (Fig. 7A).

Older dunes, probably dating to the middle Pleistocene, are exposed locally at the surface or are buried beneath younger dunes (latest Pleistocene to early Holocene) in the 3 dune fields. The older dunes and sand sheets are typically weakly cemented by the dissolution and reprecipitation of calcium carbonate to form eolianite, with reddish brown paleosols near their upper parts and a well-cemented, white-colored calcrete (also called "caliche") layer below. In the dune fields, the eolianites commonly preserve the high-angle cross-bedding of the original dunes (Fig. 7B). The younger dunes and sand sheets are typically unconsolidated, but at present they are mostly stabilized by vegetation.

Carbonate-filled root, stem, and trunk casts of fossil plants, called rhizoliths, are found in the upper parts of the older dunes. In many exposures they can be seen in their original growth position (Fig. 7C), indicating a period
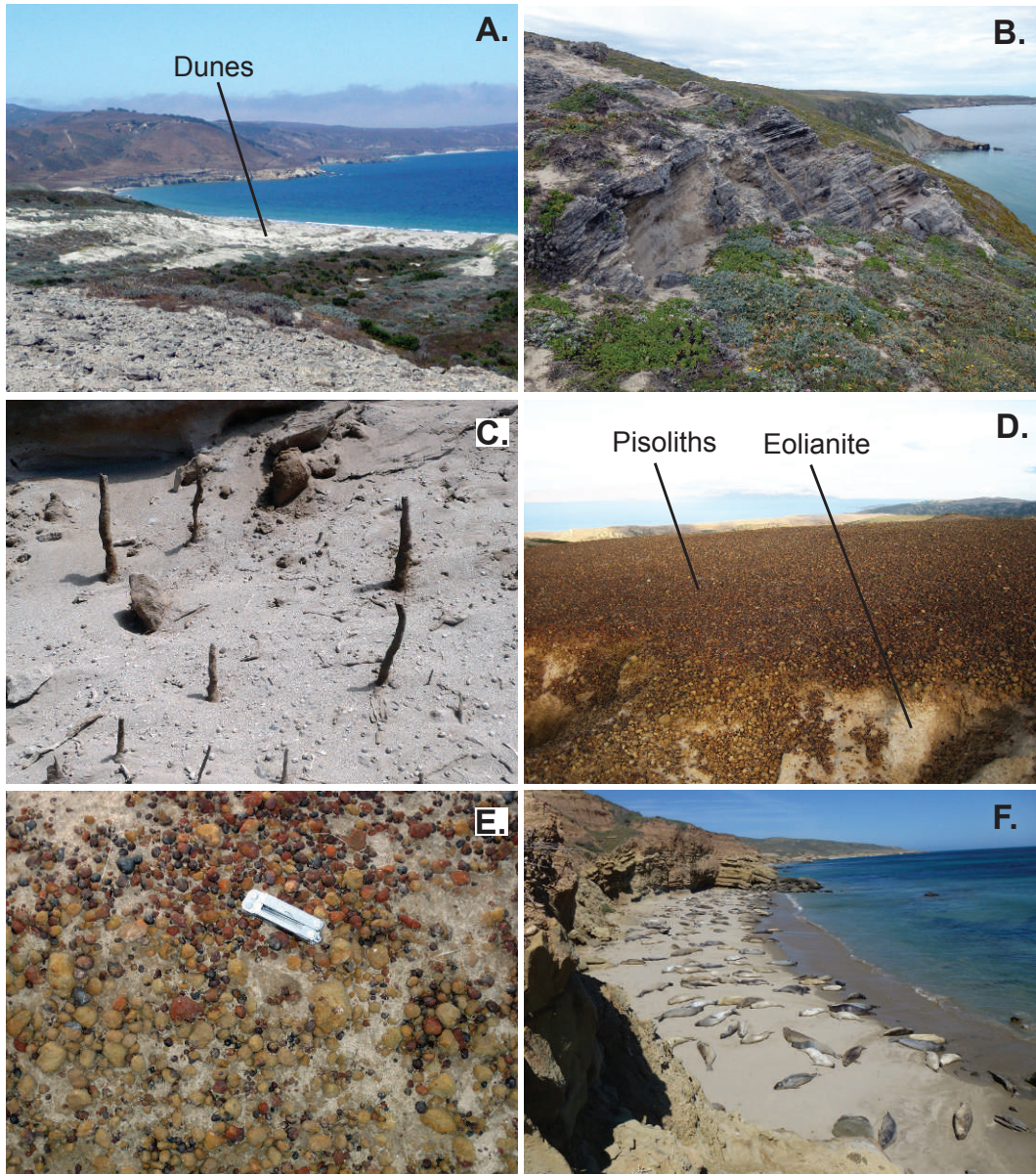
Fig. 7. (A) Climbing dunes near Skunk Point. Prevailing wind blows sand onshore and uphill (thus "climbing" dunes). (B) Eolianite, Carrington Point. Cemented sand beds are dipping away from the prevailing wind direction, indicating that this rock outcrop is a remnant of the leeward slip face of an old sand dune. In photos A and B, prevailing wind blows roughly from right to left. (C) Rhizoliths, Sandy Point. The tallest rhizoliths in the photo are roughly 30–40 cm long. (D) Pisoliths along Main Road northeast of Black Mountain. (E) Closer view of pisoliths (5 cm long pocketknife for scale). (F) Beach, near South Point. Note color contrast between calcareous beach sand and siliceous sandstone cliffs.

of dune stability in which woody tree and shrub vegetation colonized the dunes. Later, during a period of renewed dune formation and migration, sand buried the vegetation and, aided by water percolating through the dune sand,

calcium carbonate was dissolved and reprecipitated in the spaces formerly occupied by the woody plant parts, forming the rhizoliths.

In areas where older eolianite blankets the upland surface of Santa Rosa Island, reddish

brown, iron oxide–coated spherical nodules called pisoliths (Fig. 7D, 7E) are common. The pisoliths are formed by chemical weathering and biologic fixation of iron from an upper soil layer (B horizon) of the eolianite (Schulz et al. 2010). Pisoliths occur only on the older eolianite deposits, suggesting that the time required for their formation is relatively long, or that the climatic conditions required for their formation do not presently exist on SRI. Pisoliths also occur only in older eolianites on San Miguel Island (Johnson 1972) and San Nicolas Island (Vedder and Norris 1963).

Beaches

Beaches on Santa Rosa Island are important features for recreational use and wildlife habitat. For example, beaches on the Channel Islands provide important environments for pinnipeds (Fig. 7F) and seabirds, including several endemic, threatened, or endangered species (NOAA 2009). A narrow beach fringes Bechers Bay from a few hundred meters north of the pier relatively continuously to Skunk Point. On the north, west, and south coasts of the island, beaches are more commonly confined to areas that are protected from wave erosion, such as coves, bays, or inlets. Like the eolian deposits on SRI, the beach sand is composed dominantly of white to light gray calcium carbonate, which can easily be seen where beaches are adjacent to tan-colored sandstone bedrock cliffs (Fig. 7F).

Inland Landscapes

The inland area of Santa Rosa Island is a hilly, dissected terrain with elevations ranging from near sea level to 484 m at Vail Peak in the south central part of the island (Fig. 3). The Santa Rosa Island fault divides the island into topographically distinct regions. North of the SRIF, the uplifted marine terrace surface is dissected by broad, low relief, relatively widely spaced stream valleys filled with alluvium as much as 13 m thick. The alluvial fill has been incised to form near-vertical-walled arroyos, or barrancas (Woolley 1998). Several of the north-draining streams cross the SRIF and are deflected to the left, or westward, some by more than 1 km (Fig. 3). South of the SRIF, the terrain is generally more rugged, with higher elevations, more relief, higher drainage density, and deeper dissection of the steep-walled, V-shaped valleys.

The island has a radial drainage pattern, with streams draining northward, eastward, westward, and southward from the high points of Vail Peak and Soledad Mountain, located slightly south of the geographic center of the island (Fig. 3). The north–south drainage divide is shifted south of the center of the island because the part of the island south of the Santa Rosa Island fault was displaced upward by several hundreds of meters relative to the north part (Dibblee and Eherenspeck 1998), resulting in the higher elevations and more rugged terrain south of the fault.

The inland landscape regions of SRI are delineated here (Fig. 4) based on characteristics such as elevation, ruggedness (or relative flatness) of terrain, and degree of fluvial dissection (expressed as drainage density). Elevation and slope values were extracted from a LiDAR-based digital elevation model (DEM) with 1×1-m grid cells. Histograms were constructed to show the distribution of elevations and slopes for each landscape area (Fig. 8), and the shapes of the distribution curves can be related to landscape characteristics. Each value in the histogram is representative of elevation or slope for 1 m² of ground surface.

Skewness and kurtosis are 2 measures of the shape of a frequency distribution curve (histogram). Skewness is a measure of symmetry; a perfectly symmetrical distribution has a skewness of zero. An asymmetrical distribution with a long tail to the right (toward higher values) is positively skewed, whereas an asymmetrical distribution with a long tail to the left is negatively skewed. Kurtosis is a measure of how peaked or flattened the distribution appears relative to a normal (or Gaussian) distribution, which has a kurtosis equal to zero (actually, a perfect Gaussian distribution has a kurtosis of 3.0, so a term known as "excess kurtosis" subtracts 3 from this value; in this paper, "kurtosis" actually refers to "excess kurtosis"). A frequency distribution that is wider and flatter than a normal curve is platykurtic (negative excess kurtosis), which implies greater influence of the tail(s) of the distribution; a distribution that is more narrow and peaked than a normal distribution is leptokurtic (positive excess kurtosis), with greater emphasis on the central tendency of the data.

NW AREA.—The NW Area encompasses much of the island north of the Santa Rosa Island Fault, and an additional area south of

ELEVATION (m)   **SLOPE ANGLE (deg)**

NW AREA

MEAN = 142.0
S.D. = 58.9
SKEW = 0.76
KURT = 0.43

NW AREA

MEAN = 14.9
S.D. = 12.6
SKEW = 0.98
KURT = 0.29

NE AREA

MEAN = 150.4
S.D. = 67.6
SKEW = 0.84
KURT = 0.51

NE AREA

MEAN = 20.1
S.D. = 12.5
SKEW = 0.56
KURT = -0.35

SE AREA

MEAN = 129.9
S.D. = 67.8
SKEW = 0.45
KURT = -0.05

SE AREA

MEAN = 17.9
S.D. = 10.6
SKEW = 0.44
KURT = -0.22

SW AREA

MEAN = 252.4
S.D. = 87.4
SKEW = 0.004
KURT = -0.57

SW AREA

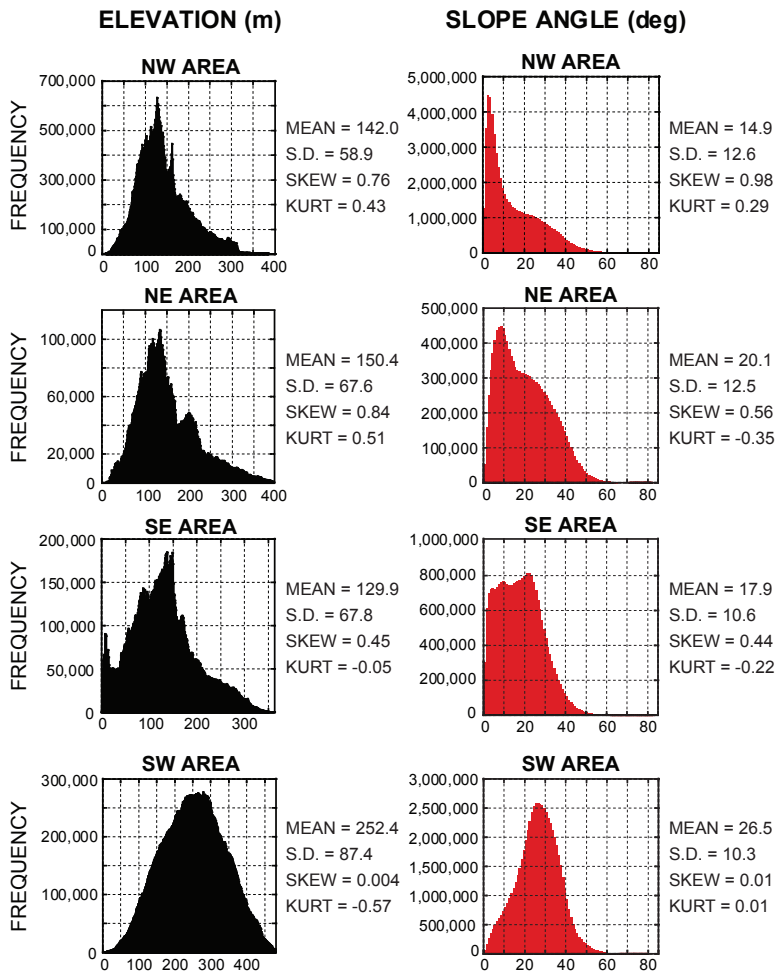MEAN = 26.5
S.D. = 10.3
SKEW = 0.01
KURT = 0.01

Fig. 8. Elevation and slope histograms, and statistical moments, for the 4 inland physiographic areas. See Fig. 4 for locations of areas.

the fault on the west side of the island (Fig. 4). Its topography is relatively flat, with a surface that slopes gently seaward, originating from an old (likely >1 Ma) marine terrace (or terraces), that has since been mantled with a layer of eolian sand as much as tens of meters thick. This surface is dissected by relatively broad river valleys containing inset alluvial terraces (Fig. 6). The crests of the interfluves, remnants of the former marine terrace surface, are broad, planar, gently sloping northward, and roughly concordant. The combined effect of marine beveling and the blanket of eolian sand gives the landscape a somewhat smooth, muted appearance; hills are typically rounded and rolling, and the planar surfaces between river valleys are relatively expansive (Fig. 9A, 9B).

Elevations range from a few meters above sea level at the modern sea cliffs to about 400 m near Black Mountain. A histogram of elevation values for this area (Fig. 8) is positively skewed (toward lower elevations) and slightly leptokurtic (many of the elevation values cluster closely about the mean elevation). The asymmetric bulge in the elevation histogram from about 70 to 120 m represents part of the sloping, planar surface typical of a marine terrace bench. The large proportion of the area that is occupied by marine terrace bench is also clearly seen in the distribution of slopes in the area (Fig. 8), which has a shape that is strongly skewed toward lower (flatter) slope values.

Another quantitative measure of landscape development is the degree of fluvial dissection
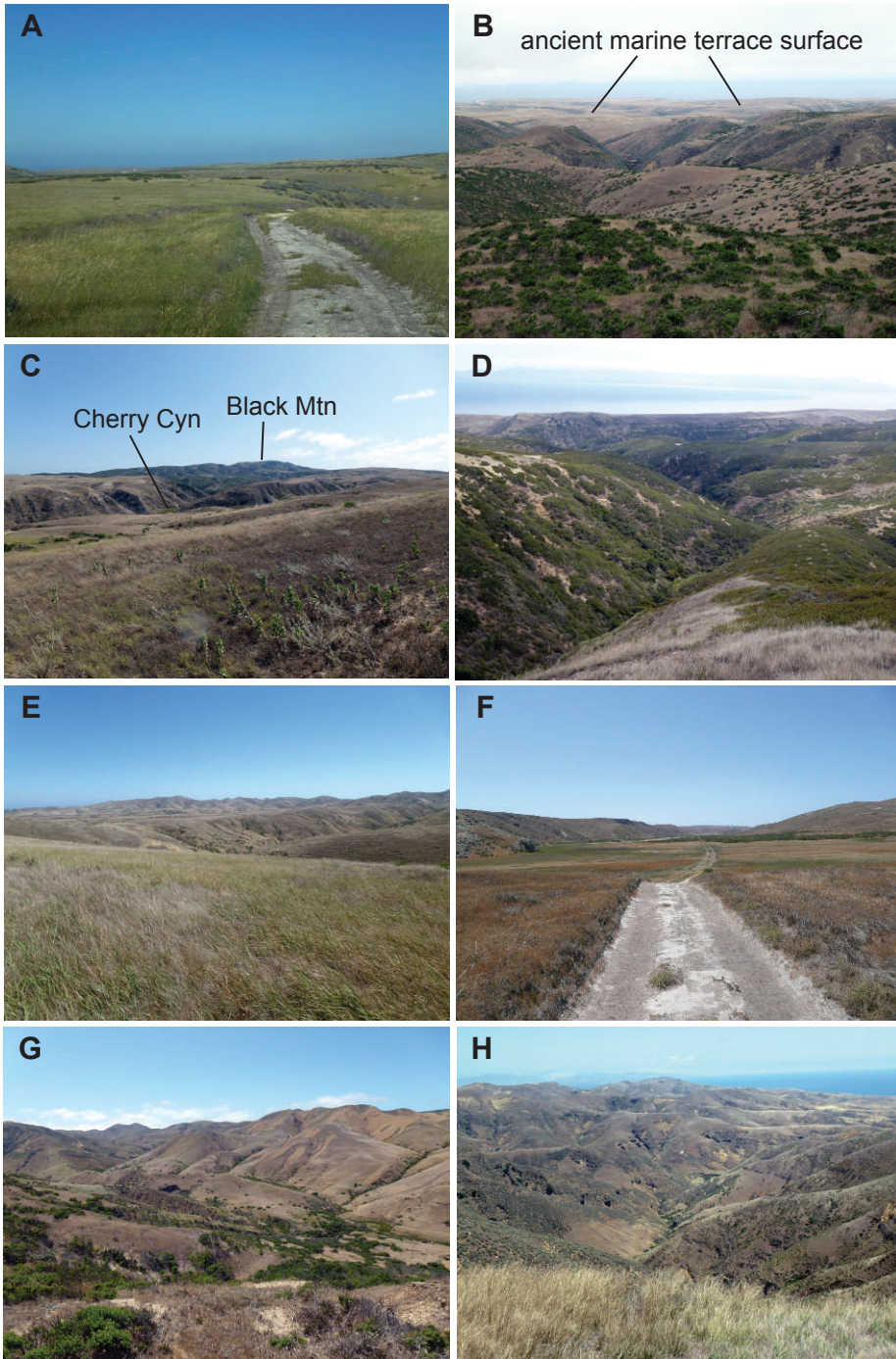
Fig. 9. Photos showing typical views of inland landscapes. (A) NW Area, ground view. (B) NW Area, view looking northward from near the center of the island. In the foreground is the rugged topography of the SW Area; the planar surface of the ancient marine terrace characterizing the NW Area is in the background. (C) NE Area, from Smith Highway looking west. (D) NE Area, looking E from the vicinity of Black Mountain. Deep, steep-walled canyons suggest relatively recent rejuvenation. (E) SE Area, sloping ridge crests in middle distance are remnants of a dissected ancient marine terrace surface. (F) SE Area, Old Ranch Canyon, looking northwest. (G) SW Area, just east of the center of the island. (H) SW Area, looking eastward down Cañada La Jolla Vieja in center of photo.

of an area, expressed as drainage density, defined as the total length of stream channels per unit area (Horton 1932, 1945, Tucker and Bras 1998). The drainage density in the NW Area is 3.6 km^{-1} (km/km^2), lowest of the 4 inland landscape areas. The streams have sinuous courses that are incised into the alluvial fill in most valleys in this area, with the notable exception of Lobo Canyon, located on the eastern side of the NW Area. The lack of significant alluvial fill in Lobo Canyon may be related to nearby recent or active uplift (see the following discussion for the NE Area), which may have caused the canyon to be flushed of the majority of its sediment rather than retaining it within the canyon, but this hypothesis requires further investigation.

NE AREA.—The NE Area extends from just east of Lobo Canyon to the inner edge of the last-interglacial marine terrace surrounding Bechers Bay. It is bounded on the south by the SRIF and on the north and west approximately by the drainage divide for eastward-draining streams (Figs. 3, 4). The elevation histogram for this area is similar to the histogram for the NW Area (Fig. 8), in that the cluster of elevation values about the mean represents the sloping, planar, old marine terrace surface, the remnants of which are expressed as concordant ridge crests (Fig. 9C). However, there is a prominent secondary peak in the tail of the positively skewed distribution that represents an area of higher elevations that may have been created by localized recent or active uplifting. The elevation distribution of this area has a higher skewness and higher kurtosis than the NW Area (Fig. 8), suggesting more diversity of topography. The mean slope in this area is about 20°, which is only slightly higher than in the NW area, but a greater area with slopes in the 20°–40° range is indicated by the positive skew and platykurtic shape of the slope distribution (Fig. 8), possibly reflecting rejuvenation and erosion in response to recent uplift.

A higher degree of fluvial dissection is indicated by a drainage density of 5.5 km^{-1}, which is the highest value for the 4 inland landscape regions delineated in this study. The valleys in the NE Area are generally steeper, deeper, and more V-shaped (Fig. 9D) than those in the NW Area. The more rugged topography and higher drainage density are strong indications that recent or active uplift is focused in this area.

As previously discussed, the observed topographic and geologic relations suggest that greater uplift has occurred south of the SRIF than north of it (Dibblee and Eherenspeck 1998). Because the fault dips to the north along its central and eastern parts, the up-to-the-south movement was likely due to normal, as opposed to reverse, sense of fault movement (Minor et al. 2012). However, the previously described south-facing escarpment, with a maximum height of ~100 m at Black Mountain, is clearly visible along the southern border of the NE Area, on the north side of the SRIF (Figs. 3, 4). Gouges or scratches along the principal slip surface of the fault, called striae, indicate that the vertical component of movement along this section of the fault has been primarily reverse slip (Minor et al. 2012). Only reverse-slip striae are present where the fault cuts across last-interglacial marine terrace deposits in the sea cliff bordering Bechers Bay, indicating that along this segment of the fault, the north side has moved upward relative to the south side during at least the past 120,000 years (Minor et al. 2012).

SE AREA.—The SE Area (Fig. 4) exhibits a mix of topographic characteristics similar to the NW and SW Areas but also has some features that are unique. The SE Area is south of the SRIF and was uplifted relative to areas north of the fault during an earlier period of tectonic activity, but the amount of uplift was considerably less than in the center of the island (SW Area). This characteristic is indicated by the lesser amount of stratigraphic offset between rock units on opposite sides of the fault (Dibblee and Eherenspeck 1998), by the overall lower topography (compare the elevation histograms for the SW and SE areas, Fig. 8), and by more rounded and smoothed topography, compared to the SW Area (Figs. 3, 4). The relatively broad, flat, and concordant ridge crests indicate that the upland surfaces of this area are uplifted remnants of an old marine terrace surface (Fig. 9E). The SE Area has the second lowest drainage density (4.5 km^{-1}) of the 4 areas. Quemada Canyon is a wide, alluvium-filled and incised drainage that resembles many of the streams and valleys in the NW Area; however, smaller stream valleys in the southern part of the area are narrower and contain significantly less alluvium. The elevation histogram for the SE Area is slightly platykurtic, reflecting many more elevations in

the range 0–100 m than exist in the other areas (Fig. 8). These lower elevations are associated primarily with Old Ranch Canyon, a very wide, straight alluvium-floored canyon that slopes gently southeastward to the ocean (Fig. 3, 9F). The first peak of the bimodal slope distribution, centered on about 10° (Fig. 8) reflects large, relatively flat areas on ridgetops, associated with remnants of old marine terrace benches, as well as the floor of Old Ranch Canyon and, to a lesser extent, fluvial terraces in Quemada Canyon. Coastal marshes at the mouth of Old Ranch Canyon are remnants of a larger estuary that occupied the lower part of the canyon in the early to middle Holocene (Cole and Liu 1994, Rick et al. 2005). The second peak in the slope distribution, centered on about 22° (Fig. 8), probably reflects steeper valley slopes in the more youthful-appearing topography of the southern part of the SE Area (Fig. 3).

SW Area.—The SW Area (Fig. 4) has the most rugged terrain on the island, with deep, steep-walled, V-shaped valleys topped by narrow ridge crests, a high degree of fluvial dissection (drainage density of 5.3 km^{-1}), and abundant landslides (Fig. 9G, 9H). The highest peaks on the island, Radar Mountain (also called Vail Peak) at 484 m (1589 ft) and Soledad Mountain at 480 m (1574 ft), are prominent features in this area. Most of the streams have cut deeper into the uplifted rocks and have steeper gradients than in the other areas, particularly in contrast to the NW Area. Ridge crests are generally sharp and narrow, as opposed to the broader and relatively flat-crested interfluves in the other areas. The elevation distribution for this area is centered about a considerably higher mean elevation than those of the other 3 areas (Fig. 8). The shape of the curve closely approaches that of a normal distribution, with skewness very near zero, although the distribution is wider and flatter (platykurtic) than a perfect normal distribution. The mean slope in the SW Area is also highest of the 4 areas at 26.5°, and the shape of the slope distribution is almost perfectly Gaussian (Fig. 8). The approximately normal shape of the elevation and slope distributions suggest a dominance of typical fluvial dissection. If there were marine terraces in this area, their topographic remnants have been eroded away due to greater overall uplift and dissection relative to the other areas. Only the largest drainages in this area have significant alluvial fill, notably Wreck, San Augustin, Water, and La Jolla Vieja canyons, and the alluvial fill is more discontinuous, occurring only in wider parts of the valleys.

FLUVIAL HISTORY

Some of the more striking landscape features on Santa Rosa Island are the incised alluvial valleys that characterize all of the north-draining streams (except Lobo Canyon) and most of the other larger streams on the island (Fig. 10A). These are wide, trough-shaped valleys that have been filled with alluvium and later incised to form steep- to vertical-walled arroyos, or barrancas, leaving a relict floodplain as much as 125 m wide and 10 or more meters above the active channel (Woolley 1998).

In several of the larger canyons, such as Cañada Verde (Fig. 10B), the alluvial fill exhibits a distinctive sequence of alternating lighter and darker layers of sediment. The darker layers generally contain silty clay or clay and organic matter, whereas the lighter-colored layers are composed primarily of silt and sand (Fig. 10B). The darker sediment may represent floodplain paleosols that developed during relatively stable and/or wetter periods (Fig. 10B, 11A), or it may represent organic-rich, low-energy channel sediments (Fig. 11B, 11C). The lighter sediments are channel-margin or floodplain aggradational deposits. Channel-fill sequences containing sand and gravel are locally found cutting into or through the floodplain deposits.

The timing and causes of the aggradation and subsequent reincision of the valleys are not well known. Charcoal near the base of the alluvial sequence in Cañada Verde yielded a calibrated radiocarbon date of approximately 29 ka, and charcoal near the base of an alluvial section in Arlington Canyon was dated at ~17 ka (Scott et al. 2010, Pinter et al. 2011). Aggradation probably continued until at least 750 years ago (Orr 1967). More detailed sampling and dating is needed to refine and expand this chronology.

Arroyos have cut through Chumash archeological sites in several locations on the island (Woolley 1998). For example, shell middens and burial sites dating to 330 yr BP (AD 1620) in Skull Gulch, on the northwest coast of the island, are cut by an arroyo, indicating that incision took place sometime after this date (Orr 1967, 1968). The earliest known photograph of
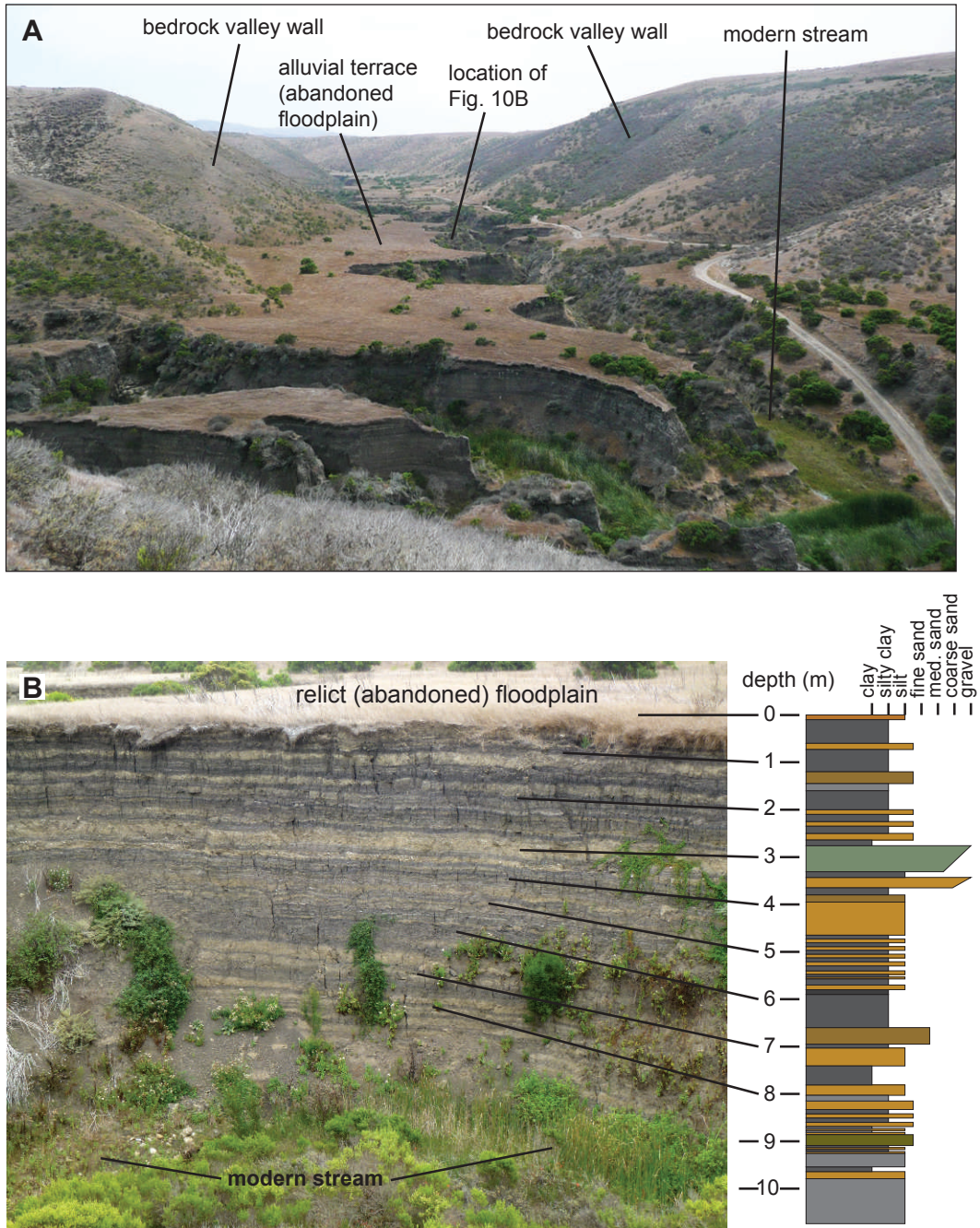
Fig. 10. (A) Cañada Verde. View looking southwest. Thickness of alluvial sediment filling the valley in the foreground is approximately 10–11 m. (B) Sedimentary deposits underlying the relict floodplain of Cañada Verde. Colors in the stratigraphic diagram approximate colors of the units. The lighter-colored layers in the photo are generally coarser grained than the darker-colored layers, which are composed primarily of clays and organic matter.

Santa Rosa Island, taken by Philip Mills Jones in 1901 during an archaeological survey (Jones 1956, reproduced in Orr 1968 and Woolley 1998), shows a well-formed barranca in Cañada La Jolla Vieja, suggesting that arroyo cutting took place prior to the beginning of the 20th
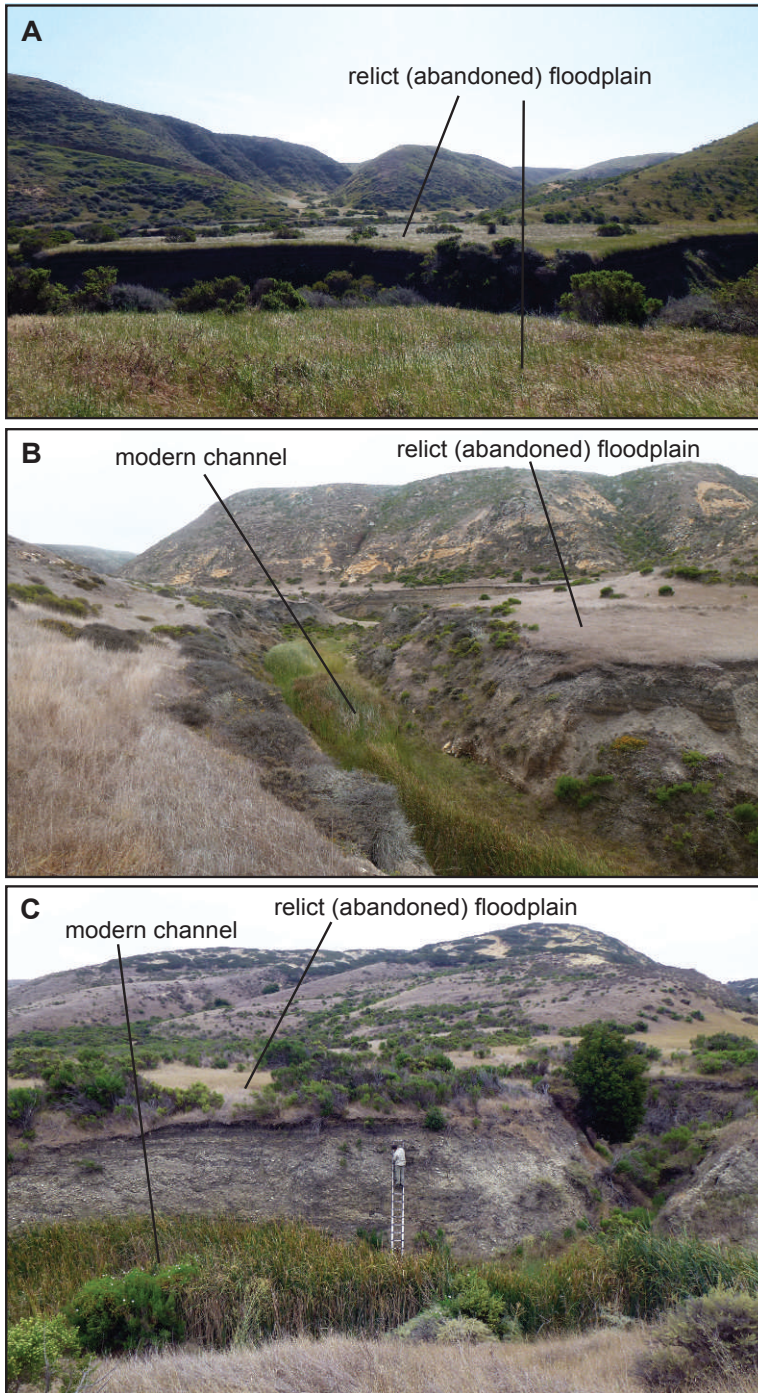
Fig. 11. (A) Lush grass growing on the floodplain produces biomass that may partially account for the darker color of some layers of alluvial sediment. (B, C) Cattails and grass grow in the modern channel of many of the streams on Santa Rosa Island. In photo C, the person is about 2 m tall. *Typha* species (cattails) in the modern channel grow to heights of 2 m or more. These are another possible source of organic material in the darker-colored sedimentary layers. Lighter-colored layers may represent drier periods or episodes of rapid sediment accumulation (such as floods), during which less organic matter accumulated in the sediment.

century. Most of the barrancas have incised the alluvial fill to bedrock (Woolley 1998).

Sedimentation rates have been estimated from cores collected from an estuarine marsh in Old Ranch Canyon (Cole and Liu 1994, Anderson et al. 2010). For the 5000 years prior to AD 1800, the sedimentation rate in the marsh was approximately 0.7 mm · year^{-1}. During the early 1800s, the sedimentation rate increased to an average of 13.4 mm · year^{-1} and peaked at 23.0 mm · year^{-1} between AD 1874 and AD 1920 (Cole and Liu 1994), which suggests increased runoff due to reduced vegetative cover caused by drought and/or overgrazing by sheep in the late 1800s. Ranching began on Santa Rosa Island in 1844, and in the 1860s and early 1870s, as many as 100,000 sheep grazed on the island (Allen 1996). Several periods of intense drought also occurred in the 1860s and 1870s. Extensive overgrazing and livestock loss due to starvation were documented on San Miguel, San Nicolas, and Santa Cruz islands following the severe drought of 1863/64 and subsequent droughts (Johnson 1980).

The increased sedimentation in the marsh reported by Cole and Liu (1994) likely resulted from increased runoff that may have also initiated arroyo cutting. Brumbaugh (1980) and Perroy et al. (2012) describe similar features on Santa Cruz Island, in which valleys cut into bedrock contain incised alluvial fills. In many of the canyons, the alluvium occurs in 2 distinct facies: a lower, fine-grained alluvium containing multiple organic-rich layers, overlain by a coarser alluvial, colluvial, and debris flow unit lacking substantial organic layers (Brumbaugh 1980). Charcoal and organics near the top of the fine-grained facies were dated to 1550 yr BP (AD 400), so the coarser-grained facies was deposited after this time, presumably due to vegetation stripping by grazing animals in the late 1800s (Brumbaugh 1980, Perroy et al. 2012). Drought and overgrazing in the late 1800s and early 1900s were also postulated to be the primary causes of severe erosion and sediment mobilization on San Miguel Island (Johnson 1980).

These data, although sparse, suggest a rough preliminary chronology for the river systems on Santa Rosa Island. Initial cutting of the river valleys would have occurred well before the Last Glacial Maximum (LGM). In fact, it is likely that several cycles of fluvial erosion and deposition would have occurred throughout the Pleistocene in response to the alternating wetter/drier periods and fluctuating sea levels of glacial/interglacial periods. Pinter et al.'s (2011) date of 29 ka for the base of alluvial fill in Cañada Verde suggests that the most recent episode of aggradation started before the onset of full glacial conditions. However, much of the aggradation may have been largely a response to rising base level, as sea level rose from its last glacial low stand of approximately 95 m below present about 20,000 years ago (Muhs et al. 2012) to its current level. Incision that created the barrancas appears to have occurred sometime between the 1600s and 1901, but the sedimentary evidence offered to date suggests that drought and overgrazing in the mid to late 1800s was a significant factor in the rapid downcutting of the arroyos.

DISCUSSION

A number of studies have attempted to relate the distributions of elevations and/or slopes to stages or processes of landscape development (e.g., Strahler 1950, 1952, 1956, Tanner 1962, Pike and Wilson 1971, Speight 1971, O'Neill and Mark 1987, Riley and Moore 1993, Montgomery 2001, Wolinsky and Pratson 2005). Landscapes develop through the processes of tectonic, isostatic, or eustatic elevation changes (in the latter case, it is sea level that changes, so the land surface elevation change is relative) and fluvial and hillslope erosional processes (Montgomery 2001)—or more simply, uplift versus erosion. If the rate of erosional downcutting equals that of uplift, the landscape is considered to be in a steady-state or equilibrium condition (Hack 1960, Montgomery 2001). Some researchers have suggested that steady-state topography might be indicated by a normal, or Gaussian, distribution of elevations or slopes, or some transformation thereof, such as log elevation or sine of slope angles (Strahler 1950, Tanner 1959, 1962, O'Neill and Mark 1987). However, few examples of pure normal distributions of slope or elevation actually have been documented. This is probably because, at least during the Quaternary, climate changes have occurred faster than many landscapes were able to adjust to them (Whipple 2001). Therefore it follows that at present, skewed distributions of elevations or slopes should be more common than normally distributed ones.

Some studies have suggested that erosional landscapes tend toward negatively skewed slope distributions, whereas actively depositional terrains display positively skewed slope distributions (Wolinsky and Pratson 2005 and references therein); however, because there are additional complexities in the system that we have not discussed here, these tendencies may not be universally true. Landscape-evolution models have been based primarily on data from continental mountain ranges, in which rainfall is the primary control on denudation rates, and base levels are local rather than absolute (i.e., sea level). In the case of the Channel Islands, however, sea level is the actual base level for the river systems, so the effect of sea-level changes is direct and unmitigated in terms of both magnitude and timing. Rapid changes in sea level, such as the transition from the LGM to the Holocene, would require rapid landscape responses, but it is not known whether there is presently enough erosive power in Santa Rosa Island's landscapes to attain a steady state in such a relatively short time. Interestingly, however, the nearly Gaussian shapes of the elevation and slope distributions of the SW Area suggest that such a rapid adjustment may indeed be possible.

An additional landscape-forming agent that was not considered in landscape development models presented to date is coastal erosion. The uplands of the NW, NE, and SE areas are partially dissected remnants of marine terrace surfaces. The process of marine terrace erosion lowered overall elevations and flattened the topography, lessening stream power and obliterating preexisting drainages. In order to recreate topography that resembles the SW Area, dissection of the marine terraces must occur through continued channel incision, which increases relief, but which also steepens valley side slopes, causing hillslope failure and slope retreat, thus widening the valleys and narrowing the interfluves. As nickpoint-driven incision progresses upstream, a network of tributary channels should also develop and grow, further disintegrating the former marine terrace surface (Anderson et al. 1999). The relatively high drainage densities of the NE and SE areas indicate that this rejuvenation and extension of the tributary networks is indeed occurring, possibly driven by tectonic uplift in the NE Area.

In the NW Area, the main drainages are filled with sediment that accumulated as sea level rose from its LGM lowstand to its current level. It appears that clearing the alluvium from the valleys must take place before significant erosion into bedrock valley floors or hillslopes can continue, which has hindered the reestablishment of steady-state topography in this area more than in the other areas. Thus, the elevation and slope distributions, along with drainage densities, depict "snapshots" of each landscape area in the process of adjusting to its unique combination of tectonic, climatic, topographic, geologic, and base-level forcings. At present, the SW Area most closely resembles a steady-state landscape, and the NW Area appears least adjusted to the most recent perturbations of its system. It should be noted, however, that this analysis is not a rigorous modeling effort, and in the interest of simplicity, we have omitted discussion of other complex factors influencing rates and processes of landscape change, such as relative erosive resistance of different bedrock types, influence of soil cover or stabilizing vegetation, and other factors.

CONCLUSION

The landscapes of Santa Rosa Island are the result of the interacting effects of geology, tectonics, and climate over long periods of time. The long-term uplift of the Channel Islands has allowed multiple marine terraces to be preserved, including the striking example surrounding Bechers Bay. Differential uplift across the Santa Rosa Island fault created high, rugged topography on the southern part of the island, but marine inundation of the northern and eastern parts formed marine terraces that have since been dissected by broad valleys containing alluvial terraces. Calcium-carbonate-rich marine sands were blown onshore from the exposed marine shelf during glacial periods when sea levels were lower, forming light-colored dunes and sand sheets. Shoreline features such as beaches and sea cliffs provide wildlife habitats and recreational opportunities for visitors to the island.

Each of these different landscapes may require different land and resource management strategies in order to optimize and balance the multiple goals of conservation, preservation, restoration, and visitor experience. It is hoped that this delineation and discussion of landscape areas will be of use in formulating plans

for future visitor trails and wilderness camp-grounds; for island restoration, construction, and management plans; in preparation of in-terpretative materials; and in identifying or guiding future natural science research needs.

LITERATURE CITED

ALLEN, K.B. 1996. Ranching on Santa Rosa Island. Pages 9–15 *in* K.B. Allen, editor, Island of the Cowboys—Santa Rosa Island. Santa Cruz Island Foundation Occasional Paper No. 7, Santa Barbara, CA.

ANDERSON, R.S., A.L. DENSMORE, AND M.A. ELLIS. 1999. The generation and degradation of marine terraces. Basin Research 11:7–19.

ANDERSON, R.S., S. STARRATT, R.M.B. JASS, AND N. PINTER. 2010. Fire and vegetation history on Santa Rosa Island, Channel Islands, and long-term environ-mental change in southern California. Journal of Quaternary Science 25:782–797.

AVILA, F.A., AND D.W. WEAVER. 1969. Middle Tertiary stratigraphy of Santa Rosa Island. Pages 48–67 *in* D.W. Weaver, D.P. Doerner, and B. Nolf, editors, Geology of the Northern Channel Islands. American Association of Petroleum Geologists and Society of Economic Paleontologists and Mineralogists, Pacific Sections, Special Publication.

BRUMBAUGH, R.W. 1980. Recent geomorphic and vegetal dy-namics on Santa Cruz Island, California. Pages 139–158 *in* D.M. Power, editor, The California Islands: pro-ceedings of a multidisciplinary symposium. Santa Bar-bara Museum of Natural History, Santa Barbara, CA.

COLE, K.L., AND G. LIU. 1994. Holocene paleoecology of an estuary on Santa Rosa Island, California. Quaternary Research 41:326–335.

CROUCH, J.K. 1979. Neogene tectonic evolution of the California Continental Borderland and western Trans-verse Ranges. Geological Society of America Bul-letin 90:338–345.

DIBBLEE, T.W., JR., AND H.E. EHERENSPECK. 1998. General geology of Santa Rosa Island, California. Pages 49–75 *in* P.W. Weigand, editor, Contributions to the geology of the Northern Channel Islands, southern Cali-fornia. American Association of Petroleum Geologists, Pacific Section, Miscellaneous Publication MP-45.

HACK, J.T. 1960. Interpretation of erosional topography in humid temperate regions. American Journal of Sci-ence 258-A:80–97.

HORTON, R.E. 1932. Drainage basin characteristics. Trans-actions of the American Geophysical Union 13: 350–361.

_____. 1945. Erosional development of streams and their drainage basins: hydrophysical approach to quantita-tive morphology. Geological Society of America Bul-letin 56:275–370.

KENNETT, D.J. 2005. The island Chumash: behavioral ecology of a maritime society. University of Cali-fornia Press, Berkeley, CA. 298 pp.

JOHNSON, D.L. 1972. Landscape evolution on San Miguel Island, California. Doctoral dissertation, University of Kansas, Lawrence, KS. 390 pp.

_____. 1980. Episodic vegetation stripping, soil erosion, and landscape modification in prehistoric and re-cent historic time, San Miguel Island, California. Pages 103–121 *in* D.M. Power, editor, The California Islands: proceedings of a multidisciplinary sympo-sium. Santa Barbara Museum of Natural History, Santa Barbara, CA.

JOHNSON, J.R., AND S. MCLENDON. 2000. The social history of native islanders following missionization. Pages 646–653 *in* D. Browne, K. Mitchell, and H. Chaney, editors, Proceedings of the Fifth California Islands Symposium. Santa Barbara Museum of Natural His-tory, Santa Barbara, CA.

JOHNSON, J.R., T.W. STAFFORD, H.O. AJIE, AND D.P. MORRIS. 2000. Arlington Springs revisited. Pages 541–545 *in* D. Browne, K. Mitchell, and H. Chaney, editors, Proceedings of the Fifth California Islands Sympo-sium. Santa Barbara Museum of Natural History, Santa Barbara, CA.

JONES, P.M. 1956. Archaeological investigations on Santa Rosa Island in 1901. Pages 201–280 *in* R.F. Heizer and A.B. Elsasser, editors, Anthropological Records 17(2). University of California Press, Berkeley, CA.

JUNAK, S., D.A. KNAPP, J.R. HALLER, R. PHILBRICK, A.A. SCHOENHERR, AND T. KEELER-WOLF. 2007. The Cali-fornia Channel Islands. Pages 229–252 *in* M.G. Bar-bour, T. Keeler-Wolf, and A.A. Schoenherr, editors, Terrestrial vegetation of California. 3rd edition. Uni-versity of California Press, Berkeley, CA.

LAJOIE, K.R. 1986. Coastal tectonics. Pages 95–124 *in* R.E. Wallace, panel chair, Active tectonics. National Academy Press, Washington, DC.

MINOR, S.A., D. BEDFORD, K.M. SCHMIDT, R.R. SCHUMANN, AND D.R. MUHS. 2012. The ups and downs of the Santa Rosa Island Fault, Northern Channel Islands, California: more than simple strike slip [abstract]. T33A-2647 presented at American Geophysical Union, San Francisco, CA; 3–7 December 2012.

MONTGOMERY, D.R. 2001. Slope distributions, threshold hillslopes, and steady-state topography. American Journal of Science 301:432–454.

MUHS, D.R., K.R. SIMMONS, G.L. KENNEDY, AND T.K. ROCK-WELL. 2002. The last interglacial period on the Pacific coast of North America: Timing and paleoclimate. Geological Society of America Bulletin 114:569–592.

MUHS, D.R., K.R. SIMMONS, R.R. SCHUMANN, L.T. GROVES, AND J.X. MITROVICA. 2012. Sea-level history during the Last Interglacial complex on San Nicolas Island, California: implications for glacial isostatic adjust-ment processes, paleozoogeography and tectonics. Quaternary Science Reviews 37:1–25.

MUHS, D.R., G. SKIPP, R.R. SCHUMANN, D.L. JOHNSON, J.P. MCGEEHIN, J. BEANN, J. FREEMAN, T.A. PEARCE, AND Z.M. ROWLAND. 2009. The origin and paleoclimatic significance of carbonate sand dunes deposited on the California Channel Islands during the last glacial period. Pages 3–14 in C.C. Damiani and D.K. Garcelon, editors, Proceedings of the Seventh California Islands Symposium. Institute for Wildlife Studies, Arcata, CA.

MUHS, D.R., J.F. WEHMILLER, K.R. SIMMONS, AND L.L. YORK. 2004. Quaternary sea-level history of the United States. Pages 147–183 in A.R. Gillespie, S.C. Porter, and B.F. Atwater, editors, The Quaternary Period in the United States. Developments in Quaternary Science, Volume 1. Elsevier, Amsterdam.

NOAA. 2009. Channel Islands National Marine Sanctuary Condition Report 2009. U.S. Department of Commerce, National Oceanic and Atmospheric Administration, Office of National Marine Sanctuaries, Silver Spring, MD. 60 pp. Available from: http://sanctuaries.noaa.gov/science/condition/cinms/download.html

NUCCIO, R.M., AND J.J. WOOLLEY. 1998. Sedimentology of the Miocene Beechers Bay Formation, Santa Rosa Island, California. Pages 91–101 in W. Weigand, editor, Contributions to the geology of the Northern Channel Islands, Southern California. Miscellaneous Publication MP-45, American Association of Petroleum Geologists, Pacific Section.

O'NEILL, M.P., AND D.M. MARK. 1987. On the frequency distribution of land slope. Earth Surface Processes and Landforms 12:127–136.

ORR, P.C. 1960. Late Pleistocene marine terraces on Santa Rosa Island, California. Geological Society of America Bulletin 71:1113–1120.

_____. 1967. Geochronology of Santa Rosa Island, California. Pages 317–325 in R.N. Philbrick, editor, Proceedings of the symposium on the biology of the California Islands. Santa Barbara Botanic Garden, Santa Barbara, CA.

_____. 1968. Prehistory of Santa Rosa Island. Santa Barbara Museum of Natural History, Santa Barbara, CA. 253 pp.

PERROY, R.L., B. BOOKHAGEN, O.A. CHADWICK, AND J.T. HOWARTH. 2012. Holocene and Anthropocene landscape change: arroyo formation on Santa Cruz Island, California. Annals of the Association of American Geographers 102:1229–1250.

PIKE, R.J., AND S.E. WILSON. 1971. Elevation-relief ratio, hypsometric integral, and geomorphic area-altitude analysis. Geological Society of America Bulletin 82:1079–1084.

PINTER, N., B. JOHNS, B. LITTLE, AND W.D. VESTAL. 2001. Fault-related folding in California's northern Channel Islands documented by rapid-static GPS positioning. GSA Today 11(5):4–9.

PINTER, N., A.C. SCOTT, T.L. DAULTON, A. PODOLL, C. KOEBERL, R.S. ANDERSON, AND S.E. ISHMAN. 2011. The Younger Dryas impact hypothesis: a requiem. Earth Science Reviews 106:247–264.

RICK, T.C., D.J. KENNETT, AND J.M. ERLANDSON. 2005. Preliminary report on the archaeology and paleoecology of the Abalone Rocks Estuary, Santa Rosa Island, California. Pages 55–63 in D.K. Garcelon and C.A. Schwemm, editors. Proceedings of the Sixth California Islands Symposium, Ventura, California, December 1–3, 2003. National Park Service Technical Publication CHIS-05-01, Institute for Wildlife Studies, Arcata, CA.

RILEY, C., AND J.M. MOORE. 1993. Digital elevation modelling in a study of the neotectonic geomorphology of the Sierra Nevada, southern Spain. Zeitschrift für Geomorphologie, Suppl. Band NF 94:25–39.

SCHULZ, M.S., D. VIVIT, C. SCHULZ, J. FITZPATRICK, AND A. WHITE. 2010. Biologic origin of iron nodules in a marine terrace chronosequence, Santa Cruz, California. Soil Science Society of America Journal 74:550–564.

SCOTT, A.C., N. PINTER, M.E. COLLINSON, M. HARDIMAN, R.S. ANDERSON, A.P.R. BRAIN, S.Y. SMITH, F. MARONE, AND M. STAMPONI. 2010. Fungus, not comet or catastrophe, accounts for carbonaceous spherules in the Younger Dryas "impact layer." Geophysical Research Letters 37:L14302, http://dx.doi.org/10.1029/2010GL043345

SORLEIN, C.C. 1994. Faulting and uplift of the northern Channel Islands, California. Pages 281–296 in W.L. Halvorson and G.J. Maender, editors, The Fourth California Islands Symposium: update on the status of resources. Santa Barbara Museum of Natural History, Santa Barbara, CA.

SPEIGHT, J.G. 1971. Log-normality of slope distributions. Zeitschrift für Geomorphologie 15:290–311.

STRAHLER, A.N. 1950. Equilibrium theory of erosional slopes approached by frequency distribution analysis. American Journal of Science 248:673–696, 800–814.

_____. 1952. Hypsometric (area-altitude) analysis of erosional topography. Geological Society of America Bulletin 63:1117–1142.

_____. 1956. Quantitative slope analysis. Geological Society of America Bulletin 67:571–596.

TANNER, W.F. 1959. Examples of departure from the Gaussian in geomorphic analysis. American Journal of Science 257:458–460.

_____. 1962. Components of the hypsometric curve of the earth. Journal of Geophysical Research 67:2841–2843.

TUCKER, G.E., AND R.L. BRAS. 1998. Hillslope processes, drainage density, and landscape morphology. Water Resources Research 34:2751–2764.

VEDDER, J.G., AND R.M. NORRIS. 1963. Geology of San Nicolas Island, California. U.S. Geological Survey Professional Paper 369. 65 pp.

VEDDER, J.G., AND D.G. HOWELL. 1980. Topographic evolution of the southern California Borderland during late Cenozoic time. Pages 7–31 in D.M. Power, editor, The California Islands: proceedings of a multidisciplinary symposium. Santa Barbara Museum of Natural History, Santa Barbara, CA.

WEAVER, D.W. 1969. Paleogeographic implications and geologic history. Pages 115–124 in D.W. Weaver, D.P. Doerner, and B. Nolf, editors, Geology of the Northern Channel Islands. Special Publication, American Association of Petroleum Geologists and Society of Economic Paleontologists and Mineralogists, Pacific Sections.

WEAVER, D.W., AND D.P DOERNER. 1969. Lower Tertiary stratigraphy, San Miguel and Santa Rosa islands. Pages 30–46 in D.W. Weaver, D.P. Doerner, and B. Nolf, editors, Geology of the Northern Channel Islands. Special Publication, American Association of Petroleum Geologists and Society of Economic Paleontologists and Mineralogists, Pacific Sections.

WHIPPLE, K.X. 2001. Fluvial landscape response time: how plausible is steady-state denudation? American Journal of Science 301:313–325.

WILLIAMS, A.P., C.J. STILL, D.T. FISCHER, AND S.W. LEAVITT. 2008. The influence of summertime fog

and overcast clouds on the growth of a coastal Californian pine: a tree-ring study. Oecologia 156:601–611.

WOLINSKY, M.A., AND L.F. PRATSON. 2005. Constraints on landscape evolution from slope histograms. Geology 33:477–480.

WOOLLEY, J.J. 1998. Aspects of the Quaternary geology of Santa Rosa Island, California. Pages 103–110 *in* P.W. Weigand, editor, Contributions to the geology of the Northern Channel Islands, Southern California, Miscellaneous Publication MP-45, American Association of Petroleum Geologists, Pacific Section.